01 Jul 2012

Concrete Surface with Nano-Particle Additives for Improved Wearing Resistance to Increase Truck Traffic

Genda Chen
Missouri University of Science and Technology, gchen@mst.edu

Dongming Yan

Chenglin Bob Wu
Missouri University of Science and Technology, wuch@mst.edu

Zhibin Lin

et. al. For a complete list of authors, see https://scholarsmine.mst.edu/civarc_enveng_facwork/963

MID-AMERICA
TRANSPORTATION CENTER

Report # MATC-MST: 441

Final Report
25-1121-0001-441

Concrete Surface with Nano-Particle Additives for Improved Wearing Resistance to Increasing Truck Traffic

Genda Chen, Ph.D., P.E., F.ASCE
Professor
Department of Civil, Architectural, and Environmental Engineering
Missouri University of Science and Technology

Dongming Yan, Ph.D.
Associate Professor
Chenglin Wu, Ph.D. Candidate
Graduate Research Assistant
Zhibin Lin, Ph.D.
Postdoctoral Research Associate
Nicholas Leventis, Ph.D.
Professor
Shruti Mahadik, Ph.D. Candidate
Graduate Research Assistant

2012

A Cooperative Research Project sponsored by the U.S. Department of Transportation Research and Innovative Technology Administration

Concrete Surface with Nano-Particle Additives for Improved Wearing Resistance to Increasing Truck Traffic

Genda Chen, Ph.D., P.E., F.ASCE
Professor and MATC Associate Director
Department of Civil, Architectural, & Environmental Engineering
Missouri University of Science & Technology

Dongming Yan, Ph.D.
Associate Professor of Civil Engineering
Zhejiang University, China
Former Post-Doctoral Fellow
Department of Civil, Architectural, & Environmental Engineering
Missouri University of Science & Technology

Chenglin Wu, Ph.D. Candidate
Graduate Research Assistant
Department of Civil, Architectural, & Environmental Engineering
Missouri University of Science & Technology
Zhibin Lin, Ph.D.
Postdoctoral Research Associate
Department of Civil, Architectural, & Environmental Engineering
Missouri University of Science & Technology

Nicholas Leventis, Ph.D.
Curators' Professor
Department of Chemistry
Missouri University of Science & Technology

Shruti Mahadik, Ph.D. Candidate
Graduate Research Assistant
Department of Chemistry
Missouri University of Science & Technology

A Report on Research Sponsored by

Mid-America Transportation Center
University of Nebraska-Lincoln
Federal Highway Administration

July 2012

Technical Report Documentation Page

1. Report No. 25-1121-0001-441	2. Government Accession No.	3. Recipient's Catalog No.
4. Title and Subtitle Concrete Surface with Nano-Particle Additives for Improved Wearing Resistance to Increasing Truck Traffic		5. Report Date July 2012
		6. Performing Organization Code
7. Author(s) Genda Chen; Dongming Yan; Chenglin Wu; Zhibin Lin; Nicholas Leventis; Shruti Mahadik		8. Performing Organization Report No. 25-1121-0001-441
9. Performing Organization Name and Address Mid-America Transportation Center 2200 Vine St. PO Box 830851 Lincoln, NE 68583-0851		10. Work Unit No. (TRAIS)
		11. Contract or Grant No.
12. Sponsoring Agency Name and Address Research and Innovative Technology Administration 1200 New Jersey Ave., SE Washington, D.C. 20590		13. Type of Report and Period Covered September 2010-March 2012
		14. Sponsoring Agency Code MATC TRB RiP No. 28471
15. Supplementary Notes		

16. Abstract

This study focused on the use of nanotechnology in concrete to improve the wearing resistance of concrete. The nano materials used were polymer cross-linked aerogels, carbon nanotubes, and nano-SiO_2, nano-$CaCO_3$, and nano-Al_2O_3 particles. As an indirect measurement of the concrete wearing resistance, the tensile and compressive properties and the permeability of concrete were evaluated for various mix designs. The optimal amount of nano material additives were determined following the American Society of Testing Methods (ASTM) standard test methodologies. The test results from the materials were compared for their mechanical behaviors. This type of technology may potentially improve the comfort level of passengers, the safety of highway operations, and the efficiency of fuel consumptions. It may also reduce the emission of CO_2 associated with the poor condition of roadways.

17. Key Words	18. Distribution Statement		
19. Security Classif. (of this report) Unclassified	20. Security Classif. (of this page) Unclassified	21. No. of Pages 42	22. Price

Table of Contents

List of Figures

List of Tables

List of Abbreviations/Nomenclature

D_{RCM} = chloride diffusion coefficient based on RCM method (unit: m^2/s);
T = average temperature at initial and final step (K);
h = test sample height (m);
x_d = chloride penetration depth (m);
t = test duration (s);
CNT = multi-walled carbon nanotubes
NS = nano-SiO_2
NC = nano-$CaCO_3$
NA = nano-Al_2O_3

Acknowledgements

Financial support to complete this study was provided by Mid-America Transportation Center under Award No. 25-1121-0001-441.

Disclaimer

The contents of this report reflect the views of the authors, who are responsible for the facts and the accuracy of the information presented herein. This document is disseminated under the sponsorship of the U.S. Department of Transportation's University Transportation Centers Program, in the interest of information exchange. The U.S. Government assumes no liability for the contents or use thereof.

Executive Summary

Both mechanical and environmental factors in highway operations can accelerate the deterioration of concrete pavements and bridge decks. To extend their service life, an attempt is made to investigate the feasibility of mixing concrete with nano materials for an improved wearing resistance of concrete surfaces. Since the wearing resistance of concrete largely depends on the strength and porosity of the concrete, the goal of this study was to characterize the strength and permeability of concrete mixed with nano materials.

To achieve the above goal, nano polymer cross-linked aerogel impregnated concrete was explored for enhanced durability, and carbon nanotubes, nano-SiO_2, nano-$CaCO_3$, and nano-Al_2O_3 impregnated concrete was tested for mechanical and physical properties. Both mechanical tests (compressive and bending) and chloride penetration tests in Sodium Chloride (NaCl) and Potassium Hydroxide (KOH) solution were conducted. Various concentrations and weights of aerogels, and various weights of nano-particles, were investigated. The compressive strength of concrete, the maximum bending load applied on simply-supported beams, the penetration depth and the diffusion coefficient of chloride ions in concrete were reported.

When mixed with mortar, Polyurea cross-linked aerogels affected the strength of the mortar by first modifying the interface bond between the sand particles and cement matrix and then absorbing water during the mortar curing process so that the effective water-to-cement ratio is reduced. As more aerogels were added into mortar, the 28-day compressive strength of the mortar without sands was significantly increased but that with sands was reduced, indicating the importance of sand particles in mortar behavior with added aerogels. The increase in compressive strength of mortar was approximately twice as much as the percentage of the aerogels added into mortar. For example, with the addition of 4% aerogels (Recipe 16) by

weight, the 28-day compressive strength of mortar can be increased by 8%. Among various aerogel concentrations considered, Recipe 16 resulted in the maximum concrete strength.

When 2wt.%-4wt.% of nano-SiO_2 particles were added to concrete, the 7-day compressive strength of concrete was increased 36.7% - 44.1% and the chloride penetration depth (permeability) was reduced 37.2% - 41.7%. The significant modifications by nano-SiO_2 are mainly due to the large surface area of these ultrafine particles. The addition of 0.1wt.% - 0.3wt.% nanotubes reduced the chloride penetration depth 15.5% – 23.3% and the compressive strength of concrete 4.4% - 17.3%. The consistent reduction in strength observed in this study seems contradictory to the positive effect of carbon nanotubes reported in the literature. It is likely attributable to the less effective dispersion of carbon nanotubes in concrete. Moderate effects of nano-Al_2O_3 and nano-$CaCO_3$ particles were observed in terms of the compressive strength of concrete and chloride penetration. For example, addition of 0.1wt.% - 0.8wt.% nano-Al_2O_3 particles increased the concrete strength 4.2% - 11.3%, and reduced the chloride penetration depth 17.8% – 31.5%. Use of 0.5wt.% - 2wt.% nano-$CaCO_3$ particles increased the concrete strength 8.1% - 9.4%, and reduced the chloride penetration depth 10.0% - 23.9%.

However, further studies are required to better understand the working principle of nano materials in concrete mixtures. Toward this end, the nanoscale structures of mixed concrete and the hydration process of cement must be examined. In addition, the unsolved issues with nano-particles dispersion in concrete, nano-particles compatibility with cement, and application cost must be addressed.

Chapter 1 Introduction

1.1 Problem Statement

The U.S. roadway transportation system is composed of nearly 600,000 bridges and 6,300,000 kilometers of streets and highways. Every year, it carries 775 billion to over 4 trillion passenger ton miles of travel and 3.8 trillion ton miles of domestic freights, close to 11% of the Gross Domestic Product (GDP). As transportation demand continues to grow, highways and bridges must be maintained and operated efficiently to ensure a steady growth of the nation's economy. In recent years, there has been a growing recognition that the construction and service of highways have a major environmental impact (Hassan, 2010), as illustrated in figure 1.1. One strategy to minimize such impact is to control the deterioration rate and thus extend the life span of existing highways and bridge decks. It can be effectively realized by improving the durability of the concrete surface that has been extensively used in highways and bridge decks.

Having a more durable road and bridge deck surface with nano material additives can facilitate the move of people and goods, meeting the ever-growing multi-mode transportation demands in the Midwest. Not only does it improve the safety in highway operations, but it also raises the comfort level of users. In addition, it will improve the efficient use of fuel energy, reducing the emission of CO_2.

1.2 Objectives of this Research

The objectives of this study are to characterize the effects of nano materials on the strength and chloride permeability resistance of concrete and to recommend one or two nanotechnologies for further investigation on their effects on other mechanical and chemical properties of concrete pavements and bridge decks. Specifically, two technical tasks will be performed to achieve the objectives:

1. Nano polymer cross-linked aerogel impregnated concrete will be explored for enhanced durability. Conventional concrete leaves behind numerous capillary pores in its cement paste once completely dehydrated. If the water trapped in the pores is removed and replaced by a solid material, the strength and durability of concrete can be improved. Toward this end, cross-linked silica aerogels (PUA X-aerogels) in its liquid form can be either sprayed and cured on existing concrete surfaces or directly mixed with concrete prior to casting. In this task, the PUA X-aerogels will be mixed with aggregates, sands, cement, and water; the mixture design will be optimized under various curing conditions for maximum mechanical strength.
2. Nanotubes, Nano-SiO_2, Nano-$CaCO_3$, and Nano-Al_2O_3 impregnated concrete will be prepared and tested for mechanical and chemical properties. In this task, four types of nano-particles will be introduced to concrete prior to casting and optimized for maximum compressive strength and permeability of concrete through experimentation.

1.3 Report Organization

This report is organized as follows: A brief review of existing studies on nano-particles and their application in concrete is provided in Chapter 2. Nano polymer cross-linked aerogels, aerogel impregnated concrete, and various mechanical tests are presented in Chapter 3. Four other nano-particles in concrete application are compared and documented in Chapter 4, which will provide a better understanding on the effects of nano-particles on the chloride permeability and compressive strength of concrete. Chapter 5 summarizes the main findings and conclusions, as well as future research needs.

Figure 1.1 Mechanical and Environmental Attacks on Modern Infrastructures

Chapter 2 Literature Review of Nano-particles in Concrete

2.1 Introduction

To date, nanotechnology applications and advances in concrete materials remain limited (Birgisson et al., 2010). Only a few marketable nano-products are commercially available. The main advances have been in the nanoscience of cementitious materials with an increase in the knowledge and understanding of basic phenomena in cement at the nanoscale. The use of nanotechnology in construction materials may also be a potential solution to the reduction of CO_2 unloading on the environment (Birgisson et al., 2010).

Recent advances in instrumentation and computational science enable scientists and engineers to obtain unprecedented information about concrete at various scales, e.g., the critical role that nanoscale structures or pore systems, as illustrated in figure 2.1, play in concrete performance and durability. This information is crucial to the prediction of the service life of concrete and to the exploration for performance improvement. Current challenges include proper dispersion and compatibility of nano materials in cement, processing and manufacturing issues, scalability, and cost. Additionally, introduction of these novel materials into civil infrastructure will necessitate an evaluation and understanding of the impact they may have on the environment and human health. What is clear, however, is that nanotechnology has changed the way that engineers look at concrete (Birgisson et al., 2010). As indicated by Gaitero et al. (2010), small changes may make a great difference in the world of concrete.

2.2 Improving Concrete Properties Using Nano Materials

2.2.1 Nano TiO_2 and SiO_2

Ozyidirim and Zegetosky (2010) studied the mechanical properties of various additives and mixtures with cementitious materials, and found that nano-silica improved the cement paste uniformity, compressive strength and elastic modulus in comparison with regular concrete and concrete containing silica fume, as indicated in figure 2.2. The permeability of concrete can also be improved to a certain extent. Results from Sanfilippo et al. (2010) showed that the addition of silica oxides into concrete can form thin films on aggregate surfaces; this effect can potentially improve the overall performance of concrete.

In addition to the improvement of compressive strength and permeability of concrete, nano-particles can increase the wearing resistivity of the concrete surface. Li et al. (2006) investigated the influence of TiO_2 and SiO_2 on concrete properties, and concluded that the abrasion resistance of concrete can be greatly improved when either nano-particles or polypropylene (PP) fibers are added. The increase in abrasion resistance of the concrete containing nano-particles is more significant. Furthermore, TiO_2 particles are more effective than SiO_2 particles for abrasion resistance enhancement. Although TiO_2 particles can trap and decompose organic and inorganic air pollutants by a photocatalytic process, ultrafine TiO_2 particles (average agglomerates of approximately 1.2 μm) unlikely affected the wear resistance of concrete surfaces (Massan et al., 2010).

2.2.2 Nano Fibers and Carbon Nanotube

Peters et al. (2010) studied the reactive powder concrete reinforced with a combination of nanocellulose and microcellulose fibers, and indicated that the fibers can benefit other micro and nano fiber reinforcement systems at a fraction of the cost. Wille and Loh (2010) studied the

effect of multiwalled carbon nanotubes on the ultimate strength, stiffness and ductility of steel fiber reinforced concrete. Mechanical characterization studies revealed that low concentrations of multiwalled nano carbon-tubes can significantly improve the bonding behavior of single pulled high-strength fibers.

2.2.3 Nano Polyurea Cross-linked Aerogels

Cross-linked aerogels have high strength and energy absorption per unit weight. Aerogels, as shown in figure 2.3(a) are monolithic, low-density, three-dimensional silica-based assemblies of nano-particles. They are environmentally sensitive (hydrophilic, fragile), and limited in practical applications due to well-defined weak points in their skeletal framework, the so-called inter-particle necks. To overcome this problem, Leventis et al. (2002; 2007) from the Missouri University of Science and Technology (Missouri S&T) have successfully attached a conformal polymer coating over the entire skeletal framework of silica aerogels, bridging the nano-particles and widening all necks. The modified aerogels are often referred to as cross-linked aerogels, as shown in figure 2.3(b).

Polyurea cross-linked aerogels prepared by reaction with Desmodur N3200 di-isocyanate did not swell under compression (Katti et al., 2006). Its stress-strain curve, as presented in figure 2.3(c), showed a short linear elastic range (< 4% strain due to polymer elasticity) followed by a ductile behavior with plastic deformation (until ~40% strain due to the reduced void space) before inelastic hardening occurs due to the nano-particle framework stiffness. The samples often experienced lateral tensile failures at approximately 77% compressive strain and 200 MPa stress. However, an apparent Poisson ratio of 0.18 was observed both in the linear elastic and the compaction regions. This observation indicates that the plastic deformation was absorbed in void

space. At the end of the compressive test, the specimen became transparent, as illustrated in figure 2.3(d) when the air in void space was removed completely.

2.3 Summary

In closure, nano materials such as cross-linked aerogels, nano-silica, and nanotubes, offered a promising solution for improving both physical and chemical properties of concrete. In this study, concrete mixed with such nano materials was tested to quantify their tensile and compressive strengths and understand the mechanism of concrete strength increases by the additives. Specifically, the effects of various types and amounts of nano-particles on the mechanical and microstructural characteristics of concrete were studied. The concrete mixture with the nano materials were compared with plain concrete to gain a basic understanding of the change in concrete material property and microstructure due to the addition of nano materials. The porosity of concrete was investigated by examining the permeability characteristics of the concrete in accordance with the standard tests of the American Society of Testing Methods (ASTM). The best practice of one or two types of nano materials are for future studies.

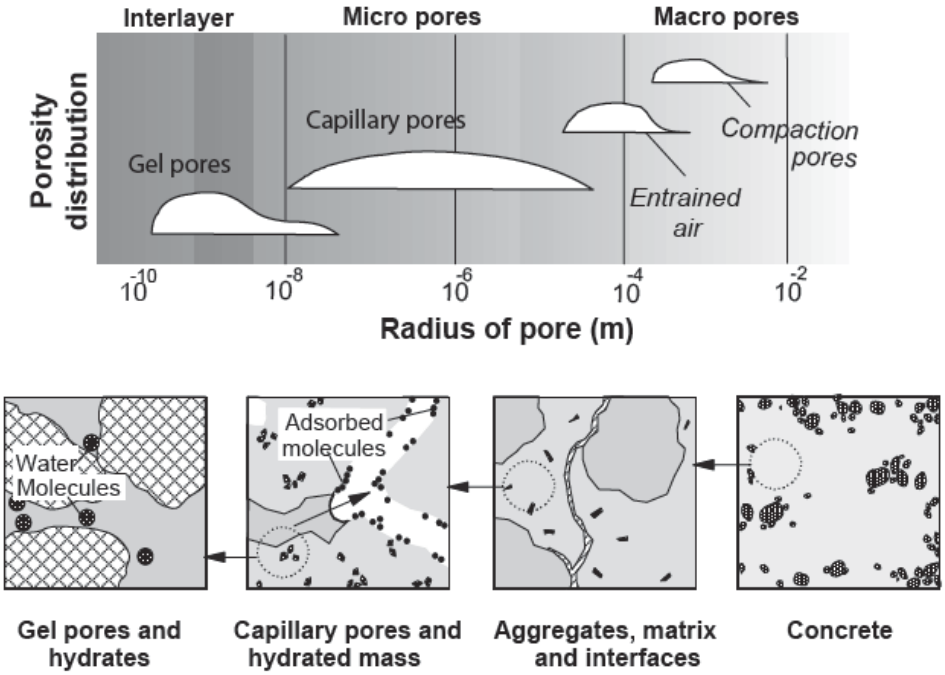

Figure 2.1 Pore Size Distribution in Cement (Maekawa et al., 2009)

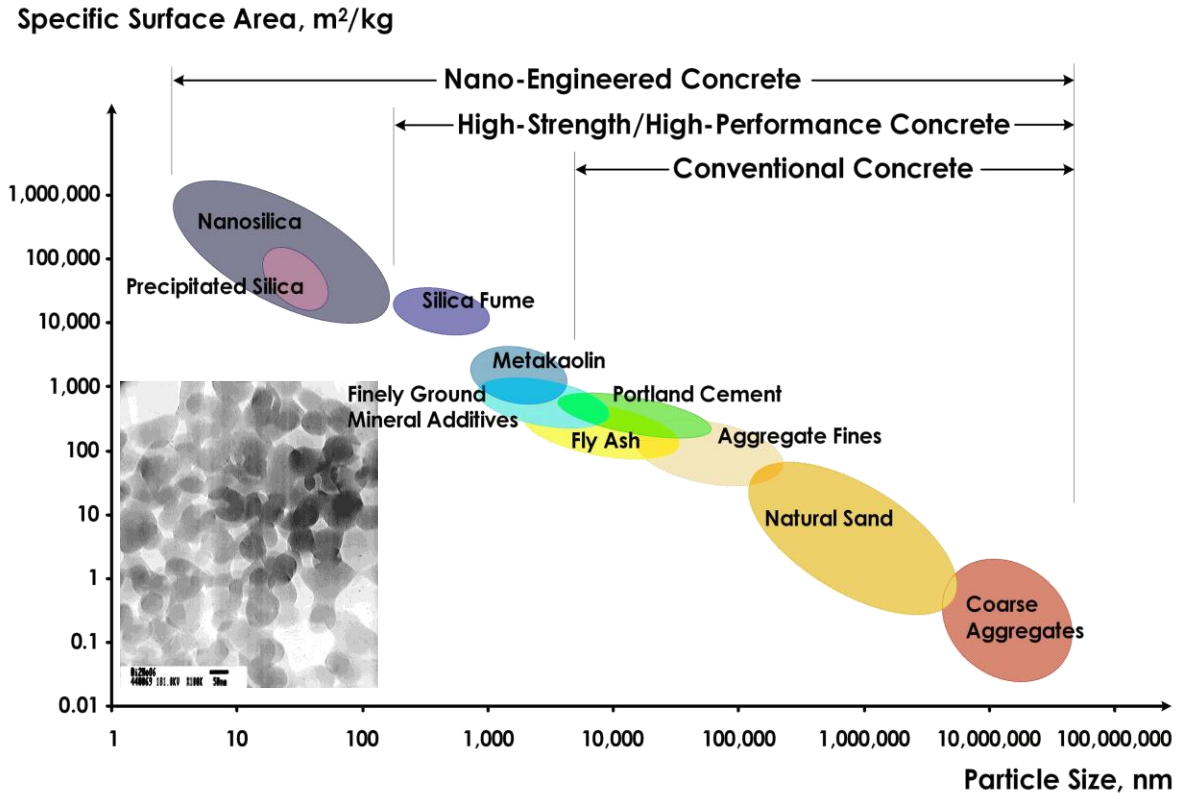

Figure 2.2 Application of Nano-SiO2 Particles in Concrete: the Particle Size-specific Surface Area Scale Related to Concrete (Sobolev et al., 2008)

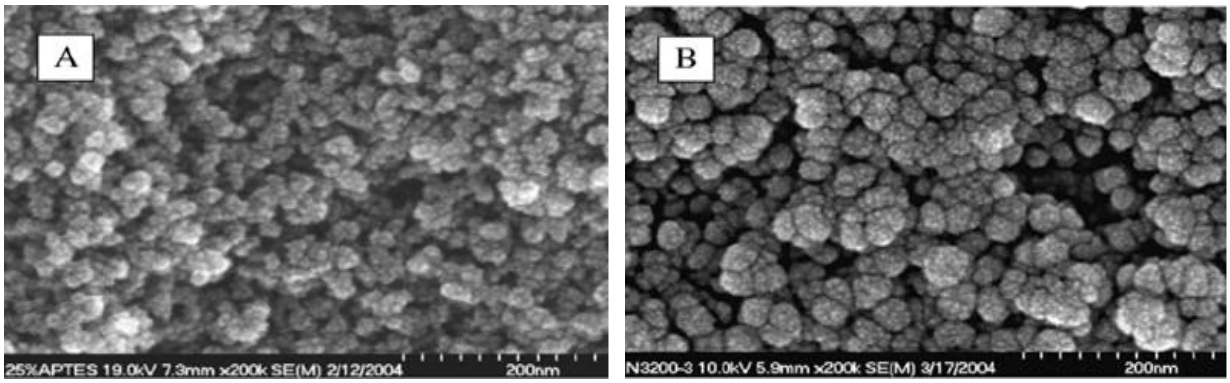

(a) General aerogels (b) Polyurea cross-linked aerogels

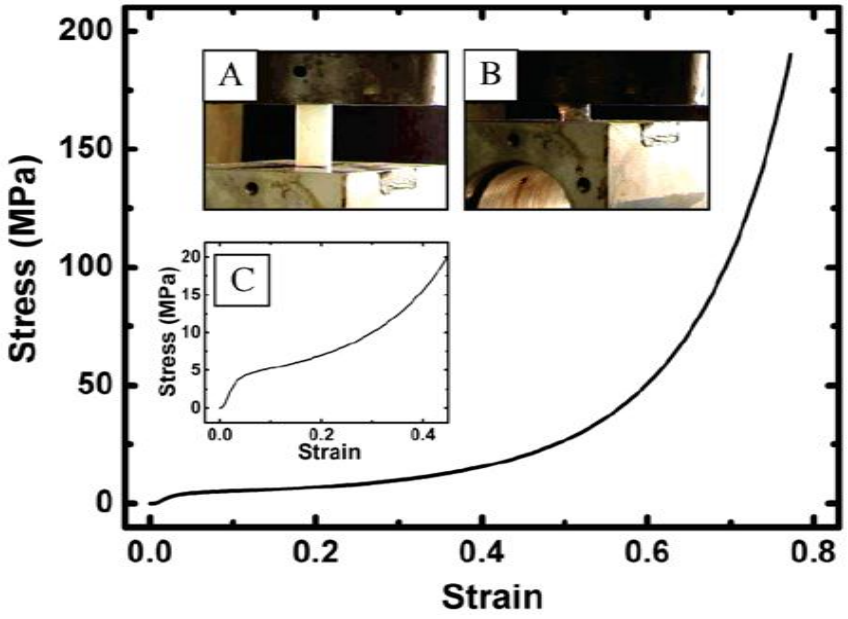

(c) Stress-strain curve under compression

(d) Transparent once compressed significantly

Figure 2.3 Polyurea Cross-linked Aerogels (Katti et al., 2006)

Chapter 3 Nano Polymer Cross-linked Aerogel Impregnated Concrete

3.1 Introduction

As shown in figure 2.3(c), Polyurea cross-linked aerogels under compression behave like steel in tension with ductile responses prior to hardening. Once mixed with concrete, the aerogels can potentially change the brittle nature and strength of mortar materials. In this section, Polyurea cross-linked aerogels were added into cement and mortar individually with different amounts by weight percentage. Mechanical properties, such as compressive and tensile strengths of the aerogels impregnated concrete, were tested with cubical, cylindrical, and slab specimens.

3.2 Experimental Program

Cubic specimens (51 mm by 51 mm by 51 mm), as shown in figure 3.1, were cast and tested according to ASTM C109/C109M-11b. The mix design of mortar cubes is 0.5 (water): 1 (cement): 2.75 (sands). The Polyurea cross-linked aerogels with a concentration rate of 0.6 g/cm^3 or Recipe 24 (Leventis et al., 2010) was selected as it most likely had the least influence on the hydration process of the Portland cement. Three types of mortar specimens: control specimens, specimens with 2% (by weight), and 4% of aerogels were added. Therefore, three types of nine specimens each were made for 7-, 14-, and 28-day strength evaluations. Three identical specimens were tested for each test condition.

To understand the interaction between aerogels and sand particles, cylindrical specimens (25 mm in diameter and 51 mm in height) were cast and tested for their mechanical strength. Aerogels with various concentrations of 0.3 g/cm^3, 0.6 g/cm^3, and 0.825 g/cm^3 were used to study the concentration effect. For convenience, three types of Polyurea aerogels were designated as Recipe 16, 24, and 33, respectively. The amount of aerogels added in the specimens was controlled at 4% by weight. As illustrated in figure 3.2(a), a set of 5 specimens

were made for each type for compressive strength tests at 28 days. The same mix proportion as mentioned for mortar cubes were used.

To understand whether the aerogel forming process influences the cement-aggregate bond that directly affects the tensile strength of mortar, slab specimens (152 mm wide, 305 mm long, 13 mm thick) with a water-cement ratio of 0.6 and aerogels with various concentrations (Recipe 16, 24, and 33) were cast and tested under three-point loading, as shown in figure 3.2(b). A set of three specimens were prepared for each type of specimen. Like cylinder specimens, 4% aerogels were added to each specimen by weight.

3.3 Test Results and Discussion

3.3.1 Mortar Cubes

The compression tests of mortar cubes were conducted on the Tinius Olsen machine. The test setup and failure mode are shown in figure 3.3. It can be observed from figure 3.3 that the mortar cubes failed in the same cone shape as often seen in regular mortar specimens. The average compressive strength of three specimens at each curing stage is presented in table 3.1. The percentage increase in 28-day compressive strength was approximately twice as much as the aerogel percentage used in the mix design of test samples. Although it is yet to be further verified, the mechanism for the observed strength changes over time is discussed here. Due to the existence of bleeding water, aerogels are formed more rapidly at the interface between aggregates and cement, potentially reducing the beneficial effect of the rough surfaces of aggregates. As a result, the link between aggregates becomes weakened and the compressive strength at its early stage is reduced. However, as both cement and aerogels are cured, the water surrounding the aggregates is significantly absorbed by the aerogels. This process can effectively

reduce the water-cement ratio, positively affect the formation of a weak interface transition zone (ITZ), and thus increase the compressive strength at 28 days.

3.3.2 Mortar Cylinders

The compressive strengths of mortar cylinders are presented in table 3.2. In general, the specimens without sand particles have lower strength than those with sand particles, likely due to the higher strength of sands. It is clearly observed from table 3.2 that, without sand particles, the compressive strength of the tested specimen increases with the addition of aerogels since the curing process of aerogels absorbs water and effectively reduces the water-cement ratio from 0.5. With sand particles, addition of a low concentration of aerogels increases the compressive strength due to the reduced water-cement ratio. Further addition of aerogels potentially forms weak links among sand particles as discussed in section 3.3.1. The net effect of the two opposite factors determines that the highest strength is achieved at a certain low (optimum) concentration of aerogels. Based on the preliminary tests in this study, Recipe 16 appears to have the optimum concentration of aerogels in terms of cost and mechanical strength.

3.3.3 Mortar Slabs

A low tensile strength mix with a water-cement ratio of 0.6 was selected to emphasize the effect of aerogels in slab specimens. Each slab specimen was tested with a three-point bending setup, as shown in figure 3.4. The average peak loads of the slab specimens with various aerogel concentrations are presented in table 3.3. It can be clearly observed from table 3.3 that the use of low concentration aerogels (Recipe 16) resulted in the maximum tensile strength of the slabs. This observation is consistent with the compressive strengths of the mortar cylinders, as given in table 3.2, and thus confirms that Recipe 16 is the right concentration for the improvement of concrete strength in civil engineering.

3.4 Concluding Remarks on Aerogels Impregnated Concrete

The preliminary tests in this study showed that, when mixed with mortar, nano polymer cross-linked aerogels can increase the compressive and tensile strength of mortar by approximately twice as much as the percentage of aerogels added by weight. For example, when 4% aerogels (Recipe 16) were added to cylinder specimens (25 mm in diameter and 51 mm tall), the compressive strength of mortar cylinders was increased by 8%. Low concentration like Recipe 16 resulted in the maximum compressive and tensile strengths of mortar based on cylinder and slab tests.

Adding aerogels into mortar potentially has two opposite effects on the mortar strength: water-cement ratio and interface between aggregates and cement. On one hand, the curing process of aerogels absorbs water from the mortar mixture, effectively reducing the water-cement ratio and increasing the mortar strength. On the other hand, aerogels are likely cured more rapidly around aggregates due to the bleeding water, forming a weak link among the aggregates and reducing the early age strength of mortar.

Table 3.1 Average Compressive Strength of Mortar Cubes with Recipe 24

Type of Specimens	3 days (MPa)	7 days (MPa)	28 days (MPa)	% increase of 28-day strength
Control with no aerogels	7.24	10.27	17.58	NA
2% aerogels added	8.41	10.07	18.27	4%
4% aerogels added	7.58	10.83	18.75	7%

Table 3.2 Average Compressive Strength of Mortar Cylinders at 28 Days

Type of Specimens	Average 28-day strength w/o sand (MPa)	Average 28-days strength w/ sand (MPa)
Control	15.86	23.64
Recipe 16	15.35	25.43
Recipe 24	20.44	19.00
Recipe 33	21.67	19.14

Table 3.3 Average Peak Load of Slab Specimens at 28 Days

Type of specimen	W/C ratio	Type of aerogels	Average 28-day peak load (N)
0.6C	0.6	NA	368
0.6P16	0.6	Recipe 16	379
0.6P24	0.6	Recipe 24	338
0.6P33	0.6	Recipe 33	285

(a) Sample preparation (b) Finished specimens

Figure 3.1 Cube Mortar Specimens

(a) 25 mm (diameter) by 51 mm (height) cylinders (b) 152 mm by 305 mm by 13 mm slabs

Figure 3.2 Cylinder and Slab Specimens

Figure 3.3 Testing of a Mortar Cube with 4% Aerogels

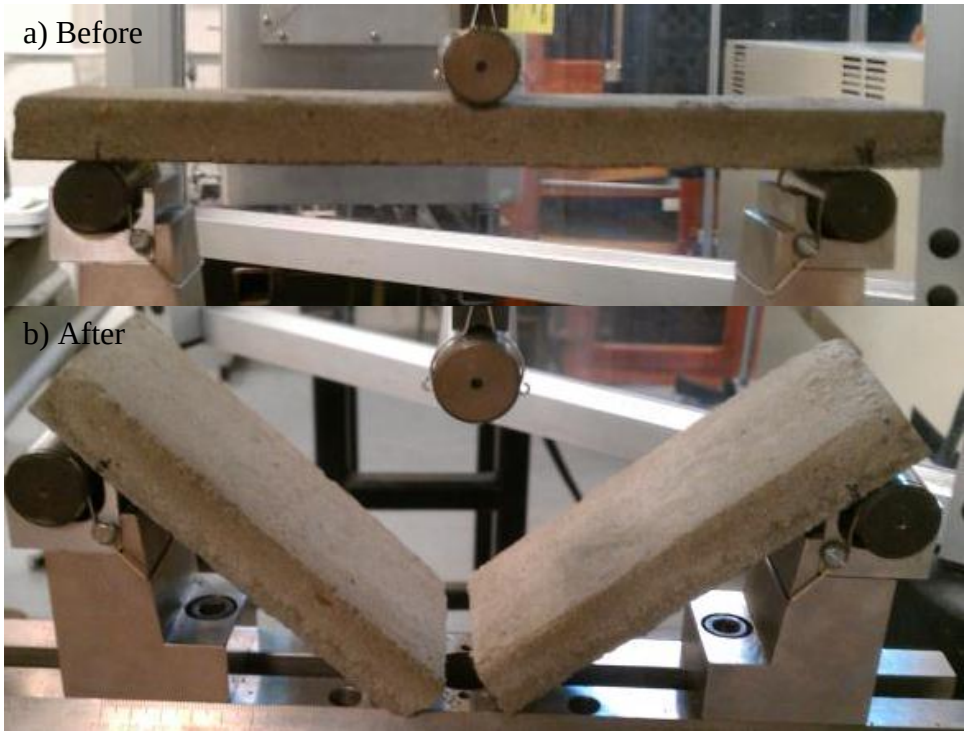

Figure 3.4 Test of a Slab Specimen

Chapter 4 Nano-particles Impregnated Concrete

4.1 Introduction

This chapter will evaluate the feasibility of introducing nano-particles into concrete for high early strength and improved durability. The durability of concrete structures is significantly influenced by the concrete permeability. The microstructure of the cement matrix is dominated by the calcium–silicate–hydrate (C–S–H) phase at the micro or nanoscale (Mehta and Monteiro, 2006). Cement/concrete properties, such as strength and durability, are basically related to the properties of the C–S–H and the porosity of concrete materials. In this study, four types of nano-particles were selected and impregnated into concrete as they potentially have different influences on the C-S-H structure or porosity. Specifically, the chloride permeability of various mixtures was examined to investigate the porosity of concrete in the micro scale.

4.2 Sample Preparation and Test Matrix

A Type-I ordinary Portland cement was used in this study. To improve workability, commercially available water reducer (Shanghai MBT& SCG High-Tech Construction Chemical Co. Ltd) was used. Graded quartz sands / aggregates and tap water were used to produce all specimens. The mixtures made with nano-particles were compared with the plain concrete with the ordinary Portland cement. Table 4.1 shows the composition data of various concrete mixtures. The sands/aggregates/cement ratio is 2/2/1 for all specimens. Most of them have a water-to-cement ratio of 0.55. The nano-particles admixtures used in this study are presented below.

4.2.1 Nano Materials

Commercial multi-walled carbon nanotubes (CNTs) (Shenzhen Nano-Tech Port Co., Ltd.) were the first nano-particle admixture used in this study. Approximately 2% of the particles by weight were sized from 20 to 40 nm in diameter and from 5 to 15 μm in length. Note that additional water in the solution should be included in the water-to-cement ratio.

Powder-type nano-SiO_2 (NS) particles (VK-SP50, HangZhou WanJing New Material Co., Ltd) were the second admixture used. Each particle was 50±5 nm in size with a fractural surface of 200±5 m^2/g.

Powder-type nano-$CaCO_3$ (NC) particles (VK-CaCY111, Xuan Cheng Jing Rui Nem Material Co., Ltd) were the third admixture used.

Commercial powder-type nano-Al_2O_3 (NA) particles (VK-L20, HangZhou WanJing New Material Co., Ltd) with a size of 10 to 20 nm and a fractural surface of 180 to 450 m^2/g were the fourth admixture used.

4.2.2 Test Matrix

Table 4.1 lists the test matrix and sample designation used in this study. The first mixture was made with Type I cement without any admixture (plain concrete). The plain concrete was used as a reference of the remaining twelve mixtures that were prepared with four types of nano-particles impregnated into the concrete. In table 4.1, CNT, NS, NC, and NA denote the carbon nanotubes, the nano-SiO_2, the nano-$CaCO_3$, and the nano-Al_2O_3 particles, respectively. The number followed by each sample designation represents the amount of nano-particles used in various mixtures by the weight of cement. For example, Sample CNT-01 denotes the concrete mixed with 0.1wt.% carbon nanotubes. Sample NS-40 includes 4wt.% nano-SiO_2 particles in the concrete mixture.

4.2.3 Mixing Procedure and Sample Preparation

A standard mixer was used for the preparation of various mixtures. Type-I Portland cement was first pre-mixed with sands/aggregates and those powder-type admixtures, as indicated in table 4.1, for 1 min. Super plasticizers and 75% water were then placed into a mixing bowl and mixed for 1.5 min. The remaining 25% water was added and mixed for an additional 30 sec. As indicated in table 4.1, the dosage of water reducer varied among test series to keep the identical workability of all samples.

In this study, compressive strength and chloride penetration tests were conducted to evaluate the compressive strength and the chloride permeability of concrete, respectively. Therefore, two types of molds were used for compressive and chloride permeability tests. The samples for compressive tests were cast with 100×100×100 mm molds. Three samples were tested at the age of 7 days and their average strength was reported. The samples for chloride penetration tests were cast with 100×160 mm PVC cylinders, as shown in figure 4.1, and then sliced into the final sizes after 7 days curing, using the HQM concrete saw cutting machine shown in figure 4.2. Note that the PVC molds were not removed as usual after 1 day curing. Instead, those PVC molds were disassembled after concrete slicing. This is mainly because concrete in the PVC mold can be sliced more precisely without any crushing edge as a result of partial confinement, as illustrated in figure 4.3. Note that the surface of samples should be totally cleansed and polished after saw-cutting. Sliced samples had a dimension of 100 by 50 mm. Three samples were tested for each condition and their average value was used. Detailed test procedures are followed by results and discussion below.

4.3 Compressive Test

Cubic samples were cured in water at a room temperature for 7 days. To investigate the effect of nano materials on the early age concrete strength, 7-day compressive tests of the concrete cubes were conducted following the ASTM C39. Each sample was loaded at 3 - 5 kN/sec. The 7-day compressive strengths are listed in table 4.2. The compressive strengths of 3 cubes were determined and their average value was evaluated and reported.

4.4 Chloride Penetration Test

The concrete permeability was investigated using the standard chloride penetration test in accordance with NT BUILD 492 (2009). Each test consisted of conditioning and measuring the electrical current, splitting the sliced sample, and measuring the chloride penetration depth.

4.4.1 Conditioning

The sample conditioning was done with a commercially available intelligent vacuum machine, creating a saturated concrete condition, as illustrated in figure 4.4. The conditioning process is identical to that used in the rapid chloride permeability test. Each sample, 100 mm in diameter and 50 mm in thickness, was first placed in a vacuum bowl and kept under a pressure of below -0.08 MPa for 3 hours. The vacuum bowl was then filled with de-aerated water to completely soak the sample and maintained in the vacuum condition for another hour. Finally, the sample was kept in the water for 18 hours under the atmospheric pressure. Note that the de-aerated water was used both for the conditioning and the preparation of KOH and NaCl solution.

4.4.2 Chloride Penetration Depth and Chloride Diffusion Coefficient

During the chloride penetration test, an electric current was applied through each test sample and chloride ions gradually penetrated through the concrete sample. Throughout the test,

both the temperature and the chloride penetration depth in each sample were recorded from which the chloride diffusion coefficient can be derived:

$$D_{RCM} = 2.872 \times 10^{-6} \frac{Th(x_d - \alpha\sqrt{x_d})}{t} \quad \text{and} \tag{4.1}$$

$$a = 3.338 \times 10^{-3} \sqrt{Th} \tag{4.2}$$

in which D_{RCM} represents the chloride diffusion coefficient (m^2/sec); T denotes the average temperature at the initial and final steps (K); h is the test sample height (m); x_d is the chloride penetration depth (m); and t represents the duration of each test (sec).

Chloride penetration tests were set up as illustrated in figure 4.5. The test setup included a test cell (schematically and graphically shown in fig. 4.6 and fig. 4.7, respectively), a data acquisition system or chloride diffusion coefficient instrument, and a PC control. Each preconditioned sample as discussed in section 4.4.1 was first placed on an oblique surface of a plastic stand in a reservoir, shown in figure 4.6, and then tied up by a clamp. The anode terminal was attached to the silicone rubber sleeve containing about 300 mL 0.2 mol/L Potassium hydroxide (KOH) solution; the cathode terminal was attached to the end cap containing about 5 L mixed solution with 5% sodium chloride (NaCl) by weight and 0.2 mol/L KOH. During the tests, the two liquid surfaces should be leveled to facilitate the ions diffusion. The temperature in the reservoir/container was recorded with a thermal probe. A potential of 30 volts applied to each sample was determined automatically by the instrument based on the initial current, as indicated in table 4.3. The data acquisition system shown in figure 4.5 was connected to the PC control and used to measure the current passed through each sample and the temperature in the container.

After the chloride test, each tested sample was broken into two halves, as illustrated in figure 4.8. The splitting surface was then sprayed with 0.1 mol/L silver nitrate solution ($AgNO_3$) to display the white color (AgCl) for about 15 minutes due to the chemical reaction of $AgNO_3$ with Cl. Therefore, the chloride ions penetration depth can be visually observed as schematically illustrated in figure 4.9 over the two splitting halves. The chloride penetration profile was determined by measuring the penetration depths at twelve locations equally spaced across the broken surface. The measured penetration depths are presented in table 4.4. With the chloride penetration depth and the measured temperature change, into equation. (4.1), the chloride diffusion coefficient can be evaluated from equation (4.1), which can be used to determine the permeability of concrete.

4.5 Test Results and Discussion

4.5.1 Compressive Strength

Table 4.2 shows the early-age compressive strength of test samples with various nano-particles. The compressive strength was derived from the average of three test samples. The standard deviation in table 4.2 of the three samples is within 3% for all samples, indicating the consistency of all test results. The effects of various nano materials on the compressive strength of concrete are discussed below.

The test samples containing 0.1wt.%, 0.2wt.%, or 0.3wt.% CNTs consistently exhibited lower strength than the plain concrete at the age of 7 days. Specifically, they reduced the compressive strength of concrete by 12.5%, 4.4%, and 17.3%, respectively. It is likely that the short CNTs were not effectively dispersed in the concrete. Without any specific treatment for nanotubes, the interface between the nanotubes and cement matrix may not be well bound. The low strength may also be attributed to the relatively high water-to-cement ratio used in concrete

mixing, which may produce a relatively low density/large pore structure and thus cause less effective development of bonding between the nanotubes and cement matrix.

As discussed in the literature, nano-SiO_2 particles have a promising effect on the strength of concrete. The 7-day compressive strengths of concrete were improved by 36.7%, 40.9%, and 44.1% when the dosages of nano-silica particles were increased by 2wt.%, 3wt.%, and 4wt.%, respectively. Unlike the concept of enhancement in physical properties through bridging and bonding the cement matrix by nanotubes, it is believed that nano-SiO_2 may significantly influence the surface property and reactivity of the processed cement. In addition, with the densification of binders due to the assistance of ultrafine particles, the improved concrete material properties, such as higher early age strength and lower permeability, can be achieved.

The NC particles did not improve the concrete strength significantly. As presented in table 4.2, the compressive strength of concrete with 0.1wt.%, 0.5wt.%, and 0.8 wt.% NC particles was only increased by less than 10% when compared with the strength of plain concrete.

Similar to NC particles, the NA particles increased the strength of concrete to a certain degree. For example, adding 0.1wt.% NA particles resulted in a 11.3% increase in early-age strength. The strength increase decreased with the increasing dosage of nano-particles. The improvement of strength due to NA particles is overall limited.

4.5.2 Chloride Permeability of Concrete with Nano-particles

The chloride penetration depths derived from the 12 measured points and their average after 4 hours of chloride diffusion tests, are given in table 4.4. The overall average chloride penetration depth of the four samples for each type of concrete mixture is summarized in table 4.5. The diffusion coefficient calculated from equation (4.1) and all the parameters in equation.

(4.1) are listed in table 4.6. The average chloride diffusion coefficient of each type of sample is summarized in table 4.7. Overall, the use of nano-particles significantly reduced the chloride diffusion coefficient of concrete samples and increased the resistance to chloride ingress in concrete, indicating the improvement of the concrete microstructure with nano-particle additives. The specific chloride penetration behaviors of various concrete mixtures are discussed below.

Table 4.5 shows an overall average chloride penetration depth of 25.2 mm or over 50 % of the sample depth in plain concrete. This result indicated that the plain concrete was a relatively high permeable and less durable material. As shown in table 4.7, the plain concrete had a chloride diffusion coefficient of 6.83×10^{-11} m^2/sec.

With the additions of 0.1wt.%, 0.2wt.%, and 0.3wt.% CNTs, the chloride penetration depths in the concrete mixture were reduced to 19.3 mm, 21.3 mm, and 21.1 mm, respectively. Although the nanotubes did not significantly improve the concrete strength, the resistances to the chloride ingress were increased by 26.6%, 19.4%, and 19.7%, respectively. In particular, 0.1wt.% nanotubes can dramatically improve the durability of concrete.

Like a significant improvement in strength, nano-SiO_2 particles can significantly improve the resistance to chloride penetration. Table 4.7 demonstrated that the chloride diffusion coefficients were 3.97, 4.19, and 3.18×10^{-11} m^2/sec when 2wt.%, 3wt.%, and 4wt.% nano-SiO_2 particles were added to concrete, respectively. These results corresponded to a 41.8%, 38.7%, and 53.4% decrease in permeability in comparison with a 6.83×10^{-11} m^2/sec for the plain concrete. The significant improvement further confirmed that the ultrafine nano-silica particles can dramatically influence the microstructure of concrete and thus affect the structural behavior, including the improved strength and resistance to the chemical ingress of chloride ions.

As discussed before, the concrete mixtures with nano-$CaCO_3$ particles increased the concrete strength by less than 10%. Similarly, their chloride diffusion coefficients were reduced by 17.3%, 35.2%, and 10.3% when 0.1wt.%, 0.5wt.%, and 0.8wt.% NC particles were added to concrete, respectively.

Similar trends were observed in the case of adding nano-Al_2O_3 particles. Specifically, the chloride ingress dramatically dropped by 18.5%, 22.3%, and 32.5% when 0.5wt.%, 1wt.%, and 2wt.% NA particles, respectively, were added to the concrete.

4.6 Concluding Remarks on Nano-particles Impregnated Concrete

The surface wearing resistance of concrete pavement can be indirectly related to concrete strength and porosity. In this chapter, the feasibility of increasing concrete strength and reducing concrete permeability or porosity by adding nano-particles was investigated. The four types of nano-particles considered include multiwall carbon nanotubes, nano-SiO_2, nano-Al_2O_3, and nano-$CaCO_3$. Preliminary test results indicated that adding a small amount of nano-SiO_2 particles into concrete can significantly increase both the concrete strength and resistance to the chloride ingress. The improvement in concrete strength and resistance to chloride penetration was moderate when a small amount of nano-Al_2O_3 or nano-$CaCO_3$ particles were added into the concrete. The addition of multiwall carbon nanotubes in concrete actually resulted in reduced concrete strength and improved permeability. The reduction in strength seemed inconsistent with the literature. The low concrete strength was attributed to the potentially ineffective particle dispersion in concrete and other uncertain factors such as the mixing quality control. Compared to plain concrete, the concrete mixed with the four types of nano-particles all had higher resistances to the chloride regress, reduced material porosity, and, therefore, more durability.

Table 4.1 Test Matrix of Concrete Mixtures (g)

Designation	PC	Aggregate	Sand	Water	Accelerator	Water reducer	Carbon nanotubes	Nano-SiO_2	Nano-$CaCO_3$	Nano-Al_2O_3
Plain	2500	5000	5000	1375	100	-	-	-	-	-
CNT-01				1250		-	125	-	-	-
CNT-02				1125		-	250	-	-	-
CNT-03				1000		-	375	-	-	-
NS-20				1375		15.0	-	50	-	-
NS-30				1375		22.5	-	75	-	-
NS-40				1375		32.5	-	100	-	-
NC-01				1375		12.5	-	-	2.5	-
NC-05				1375		17.5	-	-	12.5	-
NC-08				1375		25.0	-	-	20.0	-
NA-05				1375		12.5	-	-	-	12.5
NA-10				1375		17.5	-	-	-	25.0
NA-20				1375		20.0	-	-	-	50.0

Notes: PC = Portland cement; Plain = plain concrete with ordinary Portland cement; CNT-01, CNT-02, and CNT-03 = 0.1 wt.%, 0.2 wt.%, and 0.3 wt.% carbon nanotubes impregnated into concrete; NS-20, NS-30, and NS-40 = 2wt.%, 3wt.%, and 4wt.% nano-SiO_2 impregnated into concrete; NC-01, NC-05, and NC-08 = 0.1wt.%, 0.5wt.%, and 0.8wt.% nano-$CaCO_3$ impregnated into concrete; NA-05, NA-10, and NA-20 = 0.5wt.%, 1wt.%, and 2wt.% nano-Al2O3 impregnated into concrete.

Table 4.1 7-day Compressive Strength of Concrete Cubes

Designation	Compressive strength (MPa)				Ratio to plain concrete strength
	1	2	3	Average/Standard deviation	
Plain	8.5	8.65	9.05	8.73/0.23	-
CNT -01	7.8	7.4	7.73	7.64/0.17	-12.5%
CNT -02	8.15	8.6	8.3	8.35/0.19	-4.4%
CNT -03	7.2	7.15	7.3	7.22/0.06	-17.3%
NS-20	**11.67**	**12.04**	**12.07**	**11.93/0.18**	**36.7%**
NS-30	**12.3**	**12.59**	**12.01**	**12.30/0.24**	**40.9%**
NS-40	**12.57**	**12.58**	**12.58**	**12.58/0.00**	**44.1%**
NC-05	8.66	9.84	9.82	9.44/0.55	8.1%
NC-10	9.19	9.51	9.68	9.46/0.20	8.4%
NC-20	9.68	9.68	9.28	9.55/0.19	9.4%
NA-01	9.46	9.78	9.92	9.72/0.19	11.3%
NA-05	8.97	9.1	9.22	9.10/0.10	4.2%
NA-08	8.73	9.67	9.14	9.18/0.38	5.2%

Table 4.2 Relation Between the Initial Current and Required Test Duration

Initial current I_0 (mA)	Required test duration (hour)
$I_0 < 5$	168
$5 \leq I_0 < 10$	96
$10 \leq I_0 < 30$	48
$30 \leq I_0 < 60$	24
$60 \leq I_0 < 120$	8
$120 \leq I_0$	4

Table 4.3 Chloride Diffusion Depth

Designation	No.	Diamater (mm)	Height (mm)	Chloride diffusion depth (mm)												
				1	2	3	4	5	6	7	8	9	10	11	12	Average
Plain	1	101.1	50.0	22	21	20	20	20	25	20	25	34	30	30	28	24.6
	2	99.7	49.8	30	29	31	30	25	30	25	25	27	30	29	30	28.4
	3	100.1	49.8	22	21	20	27	30	30	24	22	25	20	28	25	24.5
	4	100.2	50.0	18	23	25	19	20	23	25	28	26	25	25	22	23.3
CNT-01	1	99.8	49.9	20	21	15	22	20	21	19	18	21	18	21	18	19.5
	2	100.8	50.1	20	20	21	19	20	20	20	21	16	22	19	18	19.7
	3	100.0	49.9	20	19	18	19	18	19	17	15	18	18	20	23	18.7
	4	101.0	49.6	22	16	17	18	21	20	18	22	19	23	18	19	19.4
CNT-02	1	100.1	49.9	22	20	20	20	21	24	17	19	19	20	24	25	20.9
	2	100.2	50.2	22	25	25	20	25	24	20	21	22	23	22	21	22.5
	3	100.0	49.9	20	19	20	18	20	24	20	19	20	22	20	25	20.6
	4	100.4	50.3	23	24	20	20	22	21	21	19	21	20	23	20	21.2
CNT-03	1	100.1	49.8	21	21	22	20	19	21	18	21	21	20	24	25	21.1
	2	100.7	49.9	20	21	22	21	20	23	24	22	22	21	22	25	21.9
	3	102.0	50.1	20	21	20	21	19	23	20	21	20	20	20	20	20.4
	4	102.0	50.0	20	19	22	20	24	23	22	20	20	21	20	21	21.0
NS-20	1	101.3	50.3	12	13	13	14	15	13	18	19	12	13	12	16	14.2
	2	101.0	49.7	19	16	16	17	15	21	19	16	15	17	14	22	17.3
	3	100.0	49.9	26	17	16	17	14	16	14	18	17	15	16	18	17.0
	4	101.0	49.9	12	10	11	9	9	11	9	10	12	10	9	12	10.3
NS-30	1	100.8	50.2	14	12	13	15	14	12	13	9	14	12	12	14	12.8
	2	100.2	49.5	16	14	12	12	13	14	18	9	15	14	14	16	13.9
	3	100.2	50.1	22	21	21	23	19	22	21	18	23	21	19	15	20.4
	4	100.8	49.8	14	13	13	13	14	12	15	14	10	13	12	14	13.1

NS-40	1	100.8	49.8	20	15	15	21	17	15	19	17	16	14	13	22	17.0
	2	100.6	50.1	23	13	10	13	12	19	22	14	16	15	16	19	16.0
	3	100.4	50.2	19	20	17	17	18	22	19	18	15	16	18	22	18.4
	4	99.7	50.0	14	9	12	11	14	13	13	12	12	11	12	10	11.9
NC-01	1	99.8	49.7	19	18	19	18	16	22	21	18	19	18	20	15	18.6
	2	100.2	49.8	20	17	20	19	17	23	16	17	18	20	16	22	18.8
	3	100.2	50.4	20	21	20	22	20	19	21	22	22	20	22	20	20.8
	4	99.8	50.3	13	18	16	18	20	22	18	18	20	17	20	22	18.5
NC-05	1	100.8	50.1	20	22	20	19	20	18	21	18	21	21	20	23	20.3
	2	100.1	49.9	15	20	20	20	16	25	22	17	20	19	20	21	19.6
	3	100.0	50.3	30	27	19	20	24	27	20	24	22	22	23	20	23.2
	4	99.8	49.6	26	23	21	24	18	22	25	20	23	15	12	20	20.8
NC-08	1	101.0	50.2	25	24	28	29	21	23	23	19	18	25	24	21	23.3
	2	99.8	49.9	25	27	18	22	22	24	23	22	21	23	20	20	22.3
	3	100.2	50.0	22	27	19	23	23	23	27	27	26	22	23	24	23.8
	4	100.1	50.0	24	22	23	24	15	19	23	20	19	22	21	23	21.3
NA-05	1	99.8	49.9	31	28	27	21	19	22	21	20	21	19	18	15	21.8
	2	100.3	49.7	25	17	20	18	22	18	18	22	20	21	16	22	19.9
	3	101.4	49.8	23	21	19	23	21	23	24	18	22	28	25	20	22.3
	4	100.4	50.3	20	16	18	19	18	21	23	18	19	18	16	21	18.9
NA-10	1	99.9	49.8	22	16	15	17	23	24	27	23	21	18	15	19	20.0
	2	101.5	50.0	25	15	22	19	24	27	23	20	20	13	17	21	20.5
	3	101.1	50.2	23	18	22	18	17	21	23	19	17	23	25	27	21.1
	4	100.3	50.1	22	18	18	13	14	18	18	20	17	15	19	18	17.5
NA-20	1	100.9	50.4	26	18	13	14	16	19	21	20	14	18	21	17	18.1
	2	101.4	50.1	20	5	17	18	20	21	23	14	19	16	23	14	17.5
	3	99.7	50.3	18	11	12	13	9	14	12	13	12	12	10	16	12.7
	4	100.6	49.9	21	20	19	18	23	21	24	25	20	17	18	22	20.7

Table 4.4 Average Chloride Penetration Depths

Designation	Chloride penetration depth (mm)					Ratio to plain concrete (%)
	1	2	3	4	Average/Standard deviation	
Plain	24.6	28.4	24.5	23.3	25.2/1.92	-
CNT-01	19.5	19.7	18.7	19.4	19.3/0.38	-23.3
CNT-02	20.9	22.5	20.6	21.2	21.3/0.72	-15.5
CNT-03	21.1	21.9	20.4	21.0	21.1/0.53	-16.3
NS-20	**14.2**	**17.3**	**17.0**	**10.3**	**14.7/2.81**	**-41.7**
NS-30	**12.8**	**13.9**	**20.4**	**13.1**	**15.1/3.11**	**-40.3**
NS-40	**17.0**	**16.0**	**18.4**	**11.9**	**15.8/2.42**	**-37.2**
NC-01	18.6	18.8	20.8	18.5	19.2/0.94	-23.9
NC-05	20.3	19.6	23.2	20.8	21.0/1.35	-16.7
NC-08	23.3	22.3	23.8	21.3	22.7/0.96	-10.0
NA-05	21.8	19.9	22.3	18.9	20.7/1.38	-17.8
NA-10	20.0	20.5	21.1	17.5	19.8/1.37	-21.5
NA-20	18.1	17.5	12.7	20.7	17.3/2.89	-31.5

Table 4.5 Raw Test Data and Calculated Chloride Diffusion Coefficient

Designation	No.	Casting date	Curing time (day)	Test date	Initial T (°C)	Final T (°C)	Duration (hour)	Height (mm)	x_d (mm)	D_{RCM} (10^{-11} m^2/sec)
Plain	1	5.19	7	5.26	21.5	22.9	4	0.0500	0.0246	6.65
	2	5.19	7	5.26	21.7	24.7	4	0.0498	0.0284	7.72
	3	5.19	7	5.26	21.7	23.3	4	0.0498	0.0245	6.61
	4	5.19	7	5.26	24.0	25.4	4	0.0500	0.0233	6.34
CNT-01	1	5.20	7	5.27	23.2	23.9	4	0.0499	0.0195	5.23
	2	5.20	7	5.27	22.3	24.3	4	0.0501	0.0197	5.30
	3	5.20	7	5.27	23.2	25.0	4	0.0499	0.0187	5.01
	4	5.20	7	5.27	22.6	24.3	4	0.0496	0.0194	5.17
CNT-02	1	5.20	7	5.27	22.8	23.5	4	0.0499	0.0209	5.62
	2	5.20	7	5.27	23.0	23.1	4	0.0502	0.0225	6.10
	3	5.20	7	5.27	22.0	23.8	4	0.0499	0.0206	5.53
	4	5.20	7	5.27	23.1	25.2	4	0.0503	0.0212	5.76
CNT-03	1	5.20	7	5.27	23.3	23.7	4	0.0498	0.0211	5.67
	2	5.20	7	5.27	23.8	25.3	4	0.0499	0.0219	5.92
	3	5.20	7	5.27	23.5	24.6	4	0.0501	0.0204	5.51
	4	5.20	7	5.27	23.7	25.1	4	0.0500	0.0210	5.68
NS-20	1	5.22	7	5.29	22.6	24.1	4	0.0503	0.0128	3.37
	2	5.22	7	5.29	22.6	23.0	4	0.0497	0.0139	3.63
	3	5.22	7	5.29	22.6	23.1	4	0.0499	0.0204	5.47
	4	5.22	7	5.29	21.9	23.1	4	0.0499	0.0131	3.42
NS-30	1	5.22	7	5.29	22.5	23.8	4	0.0502	0.0170	4.55
	2	5.22	7	5.29	22.6	22.8	4	0.0495	0.0160	4.20
	3	5.22	7	5.29	22.6	24.0	4	0.0501	0.0184	4.93
	4	5.22	7	5.29	21.8	22.5	4	0.0498	0.0119	3.08
NS-40	1	5.22	7	5.29	21.8	23.5	8	0.0498	0.0186	2.48

	2	5.22	7	5.29	21.8	22.6	8	0.0501	0.0188	2.51
	3	5.22	7	5.29	21.8	22.8	8	0.0502	0.0208	2.80
	4	5.22	7	5.29	21.8	22.8	4	0.0500	0.0185	4.94
NC-01	1	5.23	7	5.30	22.0	22.8	4	0.0497	0.0203	5.41
	2	5.23	7	5.30	22.1	23.0	4	0.0498	0.0196	5.23
	3	5.23	7	5.30	22.3	23.2	4	0.0504	0.0232	6.32
	4	5.22	7	5.29	22.1	22.9	4	0.0503	0.0208	5.62
NC-05	1	5.23	7	5.30	22.3	23.9	4	0.0501	0.0204	5.50
	2	5.23	7	5.30	22.3	24.6	4	0.0499	0.0131	3.43
	3	5.23	7	5.30	22.6	24.0	4	0.0503	0.0170	4.56
	4	5.22	7	5.29	22.6	25.0	4	0.0496	0.0160	4.22
NC-08	1	5.23	7	5.30	22.6	24.8	4	0.0502	0.0233	6.34
	2	5.23	7	5.30	22.5	23.3	4	0.0499	0.0223	6.01
	3	5.23	7	5.30	22.6	23.2	4	0.0500	0.0238	6.44
	4	5.22	7	5.29	22.5	23.3	4	0.0500	0.0213	5.73
NA-05	1	5.21	7	5.28	22.0	23.3	4	0.0499	0.0218	5.86
	2	5.21	7	5.28	22.1	23.5	4	0.0497	0.0199	5.31
	3	5.21	7	5.28	22.1	24.8	4	0.0498	0.0223	6.01
	4	5.21	7	5.28	21.8	24.3	4	0.0503	0.0189	5.09
NA-10	1	5.21	7	5.28	22.0	24.9	4	0.0498	0.0200	5.36
	2	5.21	7	5.28	21.8	23.4	4	0.0500	0.0205	5.50
	3	5.21	7	5.28	21.8	24.8	4	0.0502	0.0211	5.71
	4	5.21	7	5.28	21.9	23.0	4	0.0501	0.0175	4.67
NA-20	1	5.21	7	5.28	21.8	23.4	4	0.0504	0.0181	4.87
	2	5.21	7	5.28	21.9	23.1	4	0.0501	0.0175	4.67
	3	5.21	7	5.28	22.0	23.8	4	0.0503	0.0127	3.34
	4	5.21	7	5.28	21.9	24.6	4	0.0499	0.0207	5.56

Table 4.6 Average Chloride Diffusion Coefficients

Designation	**Chloride diffusion coefficient D_{RCM} ($\times 10^{-11}$ m^2/sec)**					**Ratio to plain concrete (%)**
	1	**2**	**3**	**4**	**Average/Standard deviation**	
Plain	6.65	7.72	6.61	6.34	6.83/0.53	-
CNT-01	5.23	5.30	5.01	5.17	5.18/0.11	-24.2
CNT-02	5.62	6.10	5.53	5.76	5.75/0.22	-15.8
CNT-03	5.67	5.92	5.51	5.68	5.70/0.15	-16.6
NS-20	**3.37**	**3.63**	**5.47**	**3.42**	**3.97/0.87**	**-41.8**
NS-30	**4.55**	**4.20**	**4.93**	**3.08**	**4.19/0.69**	**-38.7**
NS-40	**2.48**	**2.51**	**2.80**	**4.94**	**3.18/1.02**	**-53.4**
NC-01	5.41	5.23	6.32	5.62	5.65/0.41	-17.4
NC-05	5.50	3.43	4.56	4.22	4.43/0.74	-35.2
NC-08	6.34	6.01	6.44	5.73	6.13/0.28	-10.3
NA-05	5.86	5.31	6.01	5.09	5.57/0.38	-18.5
NA-10	5.36	5.50	5.71	4.67	5.31/0.39	-22.3
NA-20	4.87	4.67	3.34	5.56	4.61/0.80	-32.5

Figure 4.1 100×160 mm PVC Cylinder Mold

Figure 4.2 HQM Concrete Saw Cutting Machine

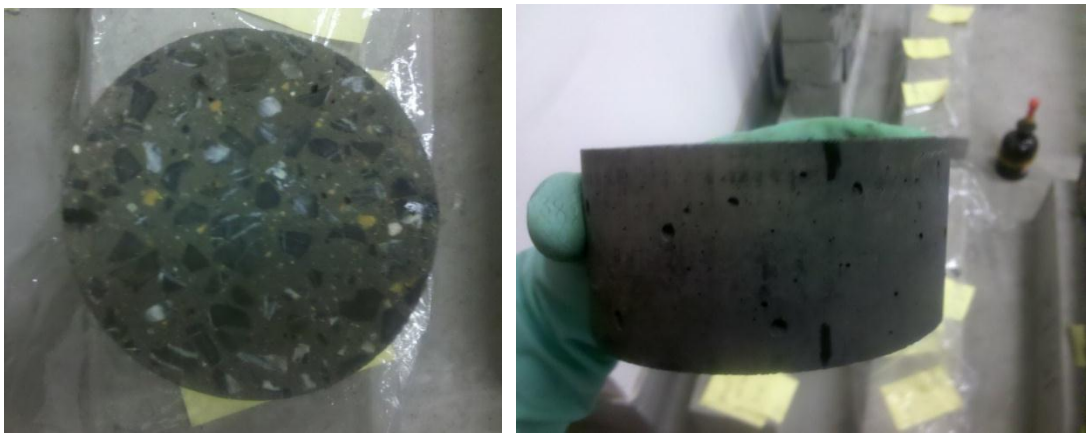

Figure 4.3 Sliced Sample with a Dimension of 100 ± l mm Diameter and 50 ± 2 mm Thickness

Figure 4.4 Intelligent Vacuum Saturated Concrete Machine

Figure 4.5 Chloride Penetration Test Setup

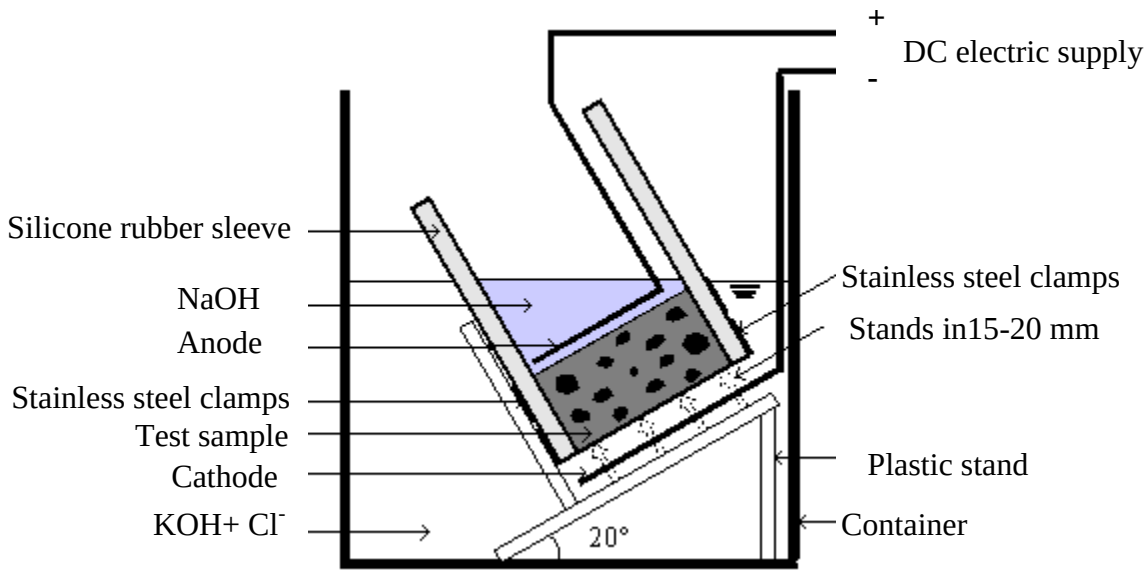

Figure 4.6 Schematics of Chloride Penetration Test Cell

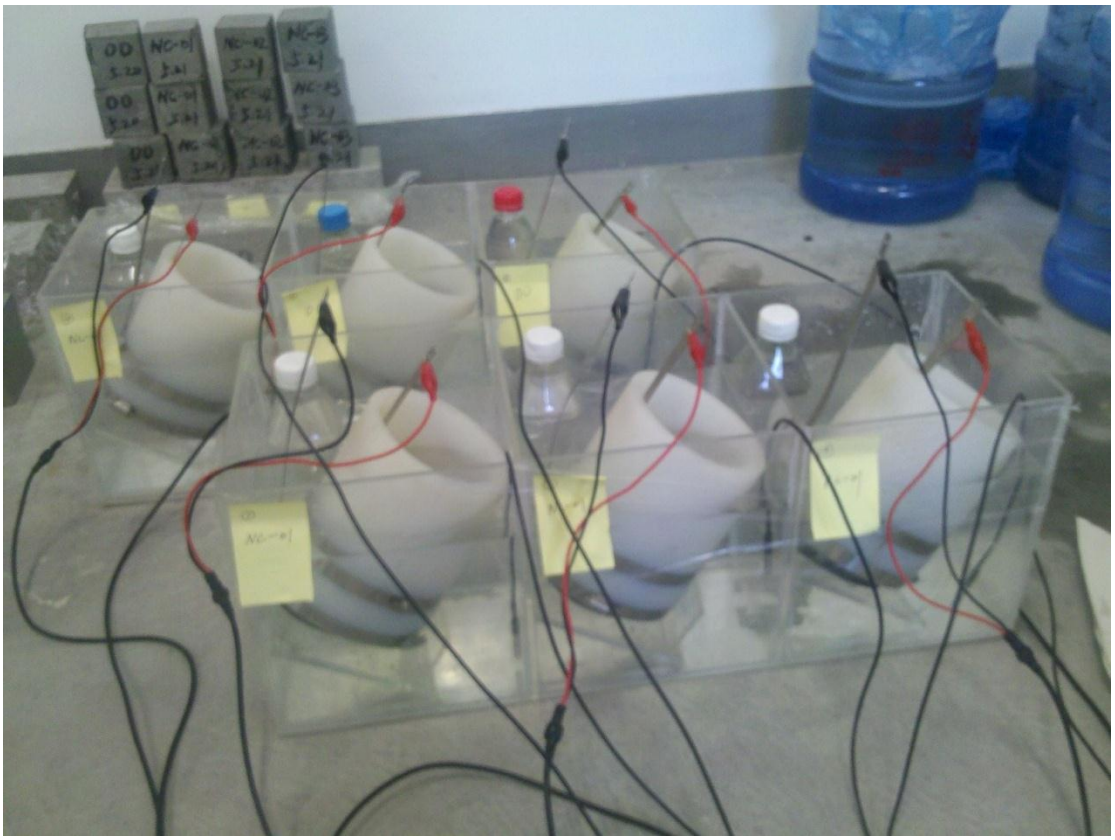

Figure 4.7 Photograph of Six Chloride Penetration Test Cells

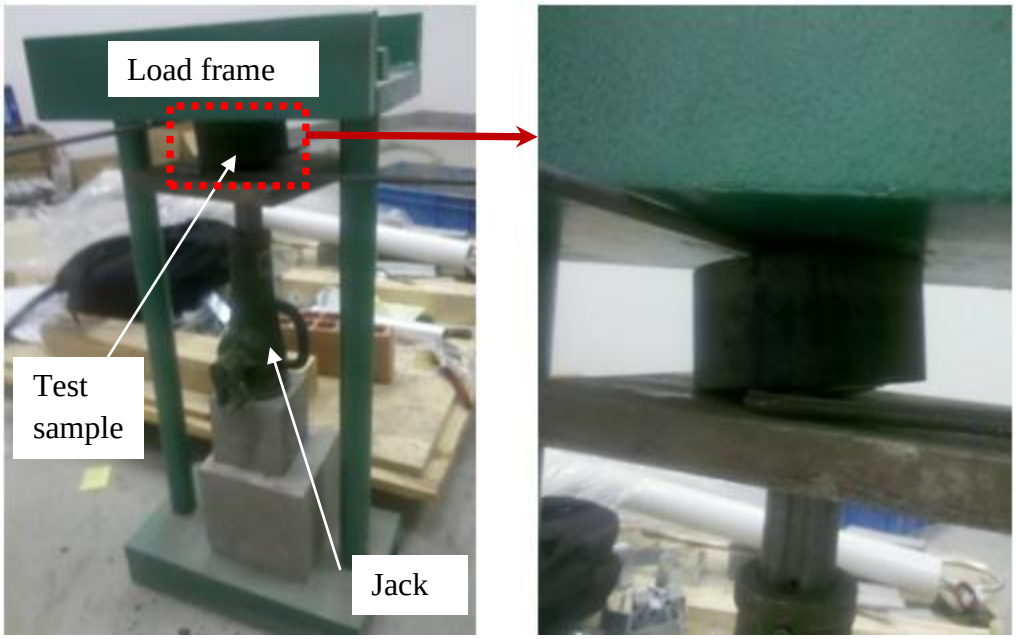

Figure 4.8 Splitting Test Setup

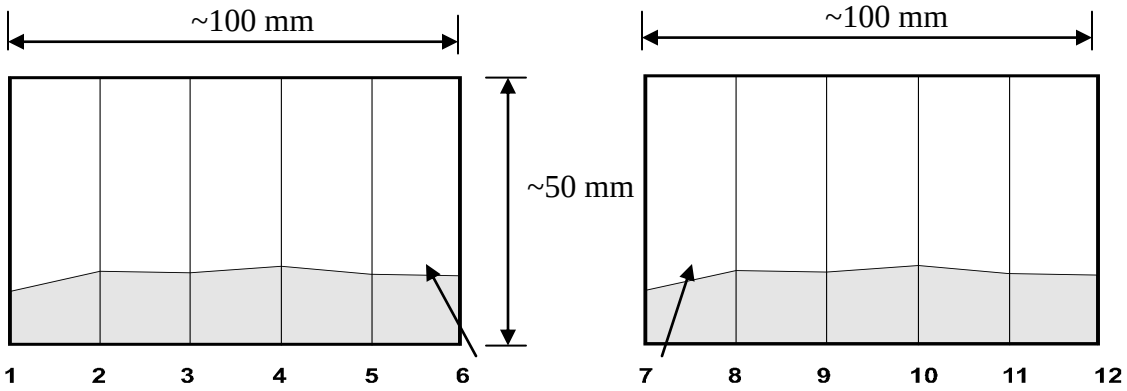

(a) One half of the broken sample (b) the one broken half

Figure 4.9 Schematics of Chloride Penetration Depth along Twelve Locations

Chapter 5 Main Findings and Recommendations

Mechanical and environmental effects in highway operations often accelerate the deterioration of highways and bridge decks. Therefore, more durable concrete materials are in great need to extend the service life of concrete pavements and bridge decks. In this report, preliminary findings and recommendations are summarized from a pilot study on the feasibility of mixing concrete with nano materials for improved strength and permeability. Specifically, mechanical and chloride penetration tests were conducted to characterize the strength and permeability of concrete mixed with five types of nano materials, including Polyurea cross-linked aerogels and nano-particles (nano-SiO_2, carbon nanotubes, nano-$CaCO_3$, and nano-Al_2O_3). Based on the experimental studies, the following conclusions can be drawn and future research issues can be identified.

5.1 Conclusions

When mixed with mortar, Polyurea cross-linked aerogels can affect the strength of the mortar by first modifying the interface bond between the sand particles and cement matrix and then absorbing water during the mortar curing process so that the effective water-to-cement ratio is reduced. The increase in compressive strength of mortar when mixed with aerogels is approximately twice as much as the percentage of the aerogels added into mortar. For example, with the addition of 4% aerogels (Recipe 16) by weight, the 28-day compressive strength of mortar can be increased by 8%.

When 2wt.%-4wt.% of nano-SiO_2 particles are added to concrete, the 7-day compressive strength of concrete can be increased by 36.7% - 44.1%. These results are consistent with what was reported in the literature. Similarly, addition of 2wt.% - 4wt.% nano-SiO_2 particles in concrete can reduce the chloride penetration depth (a direct indication of permeability reduction)

by 37.2% - 41.7%. This significant reduction in concrete permeability was mainly due to the large surface area of the ultrafine nano-particles. Therefore, nano-SiO_2 particles are a promising additive to concrete for improving the overall performance of concrete, such as early-age strength and low permeability. They can be used to potentially improve the surface wearing resistance and thus decelerate the deterioration of concrete pavements and bridge decks.

A small dosage of carbon nanotubes added into concrete may reduce the 7-day compressive strength and the permeability of concrete. The addition of 0.1wt.% - 0.3wt.% nanotubes can reduce the chloride penetration depth by 15.5% – 23.3%. The reduction in the penetration depth by the nanotubes indicates that a denser microstructure of the mixed concrete has been achieved. However, a consistent reduction of 4.4% - 17.3% in compressive strength of the three tested samples was reported in this study, which seems contradictory to the positive effect of carbon nanotubes reported in the literature. The low strength is likely attributable to the less effective dispersion of carbon nanotubes in concrete so that the interface bond between the sand particles and nanotubes is relatively weak.

Similar trends were observed in the effect of nano-Al_2O_3 and nano-$CaCO_3$ particles on the compressive strength of concrete. For example, addition of 0.1wt.% - 0.8wt.% nano-Al_2O_3 particles can increase the concrete strength by 4.2% - 11.3%, and use of 0.5wt.% - 2wt.% nano-$CaCO_3$ particles can increase the concrete strength by 8.1% - 9.4%. In terms of the chloride penetration depth, plain concrete can be improved by 17.8% – 31.5% for nano-Al_2O_3 and by 10.0% - 23.9% for nano-$CaCO_3$.

Overall, all types of the nano-particles tested in this study resulted in an increased chloride resistance of cement based materials. This is because the ultrafine nano-particles increase the surface area and promote the chemical activities surrounding the surface of

aggregates, thus dramatically improving the nanoscale structure of concrete and making the concrete more durable in highway and bridge applications.

5.2 Future Research Issues

Although promising in increasing concrete strength and resistance to the penetration of chloride ions, Polyurea cross-linked aerogels and nano-particles need to be further studied in various applications. An effective application of nano materials in concrete structures requires the advances in instrumentation and computational mechanics. In particular, the data interpretation and the working principle of nano materials in the concrete environment must be thoroughly investigated. Towards this end, the nanoscale structures or the pore system of concrete mixed with nano materials should be examined in a future study.

The hydration kinetics and mechanism of mass transport in the pore system of concrete are likely affected by impregnated nano-particles. Therefore, the influences of nano-particles on the hydration process of cement and the development of a nanoscale pore system in concrete should be studied in the future. Such information can help better predict the service life of concrete and provide new insights on how the service life can be extended. In addition, the unsolved issues with nano particles dispersion in concrete, nano particles compatibility with cement, and application cost must be addressed.

References

1. B. Birgisson, P Taylor, J. Armaghani and S P Shah. 2010. "American road map for research for nanotechnology-based concrete materials." *Transportation Research Record*, No. 2142: 130-137.

2. J. J. Gaitero, I. Campillo, P. Mondal and S. P. Shah. 2010. "Small changes can make a great difference." *Transportation Research Record*, No. 2141: 1-5.

3. M. M. Hassan, H. Dylla, L. N. Mohammadb and T. Rupnow. 2010. "Evaluation of the durability of titanium dioxide photocatalyst coating for concrete pavement." *Construction and Building Materials*, Vol. 24: 1456–1461.

4. Katti, N. Shimpi, S. Roy, H. Lu, E.F. Fabrizio, A. Dass, L.A. Capadona, N. Leventis. 2006. "Chemical, physical and mechanical characterization of isocyanate cross-linked amine-modified silica aerogels." *Chemistry and Materials*, Vol. 18: 285-296.

5. I. Flores, K. Sobolev, L. M. Torres-Martinez, E.L. Cuellar P. L. Valdez and E. Zarazua. 2010. "Performance of cement systems with nano-SiO_2 particles produced by using the sol-gel method." *Transportation Research Record*, No. 2141: 10-14.

6. N. Leventis, C. Sotiriou-Leventis, G. Zhang, and A-M. M. Rawashdeh. 2002. "Nano engineering strong silica aerogels." *Nano Letters*, No.2: 957-960.

7. N. Leventis, P. Vassilaras, E.F. Fabrizio, and A. Dass. 2007. "Polymer nanoencapsulated rare earth aerogels: chemically complex but stoichiometrically similar core–shell superstructures with skeletal properties of pure compounds." *Journal of Materials Chemistry*, Vol.17: 1502–1508.

8. H. Li, M. Zhang, J. Ou. 2006. "Abrasion resistance of concrete containing nano-particles for pavement." *Wear*, Vol. 260: 1262–1266.

9. S. Mindess, J. F. Young and D. Darwin. 2003. *Concrete*. Pearson Education, Inc. Upper Saddle River, NJ,.

10. P. Mondal, S. P. Shah, L. D. Marks, and J. J. Gaitero. 2010. "Comparative study of the effect of microsilica and nanosilica in concrete." *Transportation Research Record*, No. 2141: 6-9.

11. C. Ozyidirim and C. Zegetosky. 2010. "Exploratory investigation of nanomaterials to improve strength and permeability of concrete." *Transportation Research Record*, No. 2142: 1-8.

12. S.J. Peters, T.S. Rushing, E.N. Landis and T.K. Cummins. 2010. "Nanocellulose and microcellulose fibers for concrete." *Transportation Research Record*, No. 2142: 25-28.

13. J. M. Sanfilippo, J. F. Munoz, M. I. Tejedor, M. A. Anderson and S. M. Cramer. 2010. "Nanotechnology to manipulate the aggregate-cement paste bond effects on mortar performance." *Transportation Research Record*, No. 2142: 29-33.

14. K Wille and K. J. Loh. 2010. "Nano-engineering ultra-high-performance concrete with multiwalled carbon nano-tubes." *Transportation Research Record*, No. 2141: 10-14.

15. K. Sobolev, I. Flores, R. Hermosillo and L.M. Torres-Martínez. 2006. "Application of nanomaterials in high-performance cement composites; Proceedings of the ACI Session on Nanotechnology of Concrete: Recent Developments and Future Perspectives." Edited by K. Sobolev and S.P. Shah, Denver, USA, ACI SP-254, 2008, pp. 93-120.

16. American Society of Testing Methods. 2011. "Standard Test Methods for Compressive Strength of Hydraulic Cement Mortars." *American Society of Testing Methods* (ASTM), A370.

17. N. Leventis, C.S. Leventis, N. Chandrasekaran, S. Mulik, Z. J. Laromore, H. Lu, G. Churu, and J. T. Mang. 2010. "Multifunctional polyurea aerogels from isocyanates and water: a structure-property case study." *Chemistry and Materials*, Vol. 22: 6692-6710.

18. Mehta P, and Monteiro P. 2006. "Concrete Microstructure Properties and Materials." 3rd ed. Mc-Graw Hill Companies Inc.